

<https://doi.org/10.1038/s41746-025-01690-3>

Wearable fNIRS platform for dense sampling and precision functional neuroimaging



Ali Rahimpour Jounghani^{1,4}, Anupam Kumar^{2,4}, Laura Moreno Carbonell^{1,3,4}, Ester Patrizze Lopez Aguilar¹, Tulla Bee Picardi¹, Seth Crawford², Audrey K. Bowden² & S. M. Hadi Hosseini¹

Precision mental health aims to improve care by tailoring interventions based on individual neurobiological features. Functional near-infrared spectroscopy (fNIRS) is a cost-effective and portable alternative to traditional neuroimaging, making it a promising tool for this purpose. This study evaluates a self-administered, wearable fNIRS platform designed for precision mental health applications, focusing on its reliability and specificity in capturing individualized functional connectivity patterns. The platform incorporates a wireless, portable multichannel fNIRS device, augmented reality guidance for reproducible device placement, and a cloud-based system for remote data access. In this proof-of-concept study, eight adults completed ten dense-sampled sessions involving cognitive tasks and resting-state measurements. Results demonstrated high test-retest reliability and within-participant consistency in functional connectivity and activation patterns. These findings support the platform's feasibility for individualized functional mapping. Future research with larger and more diverse cohorts, including clinical populations, is necessary to explore its potential for disorder-specific applications.

Mental illnesses affect approximately one in three individuals during their lifetime¹. However, more than half of those affected may not receive adequate care due to challenges in diagnosis or accessing appropriate treatment². Despite advancements in mental health care, current clinical practices in psychiatry heavily depend on structured interviews and patient self-reports for diagnosis and treatment monitoring³. These methods, largely based on the Diagnostic and Statistical Manual of Mental Disorders (DSM-5), offer symptom-based categorizations but lack objective, biologically informed diagnostic criteria^{4,5}. Additionally, the significant heterogeneity of psychiatric conditions, coupled with the complexity of their subtypes⁶, underscores the limitations of traditional approaches that apply uniform treatment paradigms. Addressing these challenges requires novel strategies that prioritize personalized, biologically grounded methods of assessment and intervention.

To address this challenge, there has been a notable increase in the pursuit of personalized healthcare in recent years, particularly evident in the field of mental health^{7–9}. This shift reflects a growing tendency to move beyond conventional care delivery paradigms and standards of one-size-fits-all towards the adoption of tailored diagnoses and treatments. Amidst

this evolving landscape, the concept of “precision mental health” has surfaced as a central focus within the broader scope of personalized medicine⁸. It aims to facilitate a more nuanced and analytical diagnosis and customize interventions more accurately based on patient-specific phenotypes, thereby enhancing the efficacy of mental healthcare⁹. Moreover, it underscores the necessity of moving away from relying solely on traditional self-reported data and understanding the biological basis of mental disorders to provide an empirical basis for clinical psychiatric decisions. This emerging model of precision psychiatry aims to address challenges in enhancing disease classification and improving diagnostic precision. However, translating this promise into improved clinical outcomes requires further empirical validation.

Functional magnetic resonance imaging (fMRI) has revolutionized our understanding of human brain function over the past three decades¹⁰, yet its integration into mental health clinics remains limited. While fMRI offers crucial insights into brain activity, its reliance on group-average activation maps can obscure individual-specific patterns, which are critical for understanding the heterogeneous nature of mental illnesses^{11–15}. To accurately measure individual differences in brain activity, it is imperative to

¹Department of Psychiatry and Behavioral Sciences, School of Medicine, Computational Brain Research and Intervention (C-BRAIN) Laboratory, Stanford University, Palo Alto, CA, USA. ²Department of Biomedical Engineering, Vanderbilt University, Nashville, TN, USA. ³Department of Bioengineering, Stanford University, Palo Alto, CA, USA. ⁴These authors contributed equally: Ali Rahimpour Jounghani, Anupam Kumar, Laura Moreno Carbonell.

e-mail: hosseiny@stanford.edu

ensure the reliability and specificity of the measuring system by identifying the factors that affect reliability and evaluating how they influence measurement variability. Moreover, traditional fMRI studies often rely on short measurement durations, which may not capture the full variability of brain activity and can lead to less reliable results¹⁰.

Previous research highlights the importance of individualized approaches, revealing unique patterns of brain activity and variability in functional organization across individuals^{11–16}. Moreover, as Gordon et al.¹² demonstrated, the precision functional mapping of individual human brains requires dense-sampled fMRI data to reliably identify individual-specific brain activity. However, the cost and practical limitations of fMRI restrict the collection of dense-sampled data (i.e., collecting a large amount of data over multiple sessions, providing a more comprehensive and reliable view of brain data) necessary for reliable diagnosis and classification in psychiatric patients^{11,12,17}. To address these challenges, functional near-infrared spectroscopy (fNIRS) has emerged as a promising optical functional brain imaging alternative^{18–20}. With its affordability, portability, and tolerance to motion artifacts, fNIRS offers a viable solution for studying brain function in naturalistic settings^{21,22}. Concurrent fNIRS-fMRI studies have demonstrated strong agreement between the two methods, affirming the reliability and utility of fNIRS in psychiatric research^{23–26}.

By providing localized brain data detection and greater tolerance to noise and movement compared to other portable brain imaging techniques such as electroencephalography (EEG), fNIRS presents significant advantages for studying psychiatric populations^{22,27,28}. Its compatibility with clinical bedside studies further enhances its appeal, offering a valuable tool for investigating neurological conditions and psychiatric disorders²¹. With its ability to capture task-driven activations and reproduce patterns of brain activity observed in fMRI, fNIRS holds promise for advancing our understanding of mental illnesses and improving clinical care.

Despite the advancements and potential of fNIRS, there are significant technical and administrative gaps in current systems that hinder their widespread adoption in psychiatric research and patient care. Existing fNIRS systems are often cumbersome, wired, and designed for administration by a technician in the lab settings, posing challenges for at-home or remote monitoring. To address these gaps and in pursuit of integrating functional neuroimaging into psychiatric clinics, we have developed a multichannel fNIRS imaging system which is the extension of our single-channel device²⁹. Designed for easy and comfortable use at home, this system facilitates the collection of dense-sampled prefrontal cortex (PFC) data. This system is integrated in a platform that features (a) an intuitive tablet application that utilizes augmented reality (AR) enabled by the tablet camera to guide users through proper and reproducible device placement, (b) a set of app-integrated cognitive tests specifically designed and curated for the tablet, and (c) wireless synchronized recordings of both cortical brain activity and behavioral responses. All data are securely stored in a HIPAA-compliant cloud solution, allowing clinicians to remotely monitor patients' brain responses and cognitive outcomes through a user-friendly web portal.

Therefore, our proposed wearable fNIRS platform provides a cost-effective, wireless, and portable functional brain imaging solution, enabling unsupervised, dense-sampling of brain activity in naturalistic settings (e.g., at home, school or office). This allows for remote monitoring and more accurate representation of brain function during daily activities, which is crucial for precision mental health. Moreover, the augmented reality-guided (AR guided) placement procedure enables remote unsupervised data collection in a consistent and reproducible manner. Although the platform includes AR functionality for guiding proper and reproducible device placement, this feature was developed post hoc and was not utilized during the current study. Manual placement following the standard 10–20 system was employed for this dataset. Finally, the cloud-based data management and tablet-based standardized cognitive tests synced with brain activity measurements enhance usability and scalability, paving the way for integration into routine clinical practice and large-scale studies.

The validation of the proposed system holds significant potential for clinical impact in psychiatry, marking a departure from the current

paradigm of small-scale neuroimaging studies conducted solely in laboratory settings. This advancement paves the way for large-scale, population-based cohort studies conducted in real-world settings, enabling the identification of both common patterns across individuals and those consistently present in specific individuals. This approach would facilitate capturing the heterogeneity of each illness, potentially revealing previously unknown subtypes and generating new hypotheses regarding their etiology. By enabling the collection of extensive brain data, the system facilitates the identification of reliable and reproducible patterns in individuals, thereby accelerating the development of effective biomarkers that are ecologically valid and suitable for clinical applications. These biomarkers can either supplement or replace standard, descriptive measurements, facilitating diagnosis and early detection of mental illnesses. Additionally, such characterization is essential for informing the development of effective treatments to slow or stop mental illness and preserve brain function, as different subgroups may respond differently to a given drug. Ultimately, the ability to capture brain patterns in an ecologically valid condition (e.g., at home) will enhance the monitoring of treatment response.

Longitudinal sessions involving the same individuals can help standardize certain sources of variation, thus offering more appropriate data for assessing the reliability of the measuring system^{30,31}. Therefore, reliability and specificity stand as crucial concerns in functional activation measurements, as the ability to discern individual differences may be compromised if the method's reliability and specificity are uncertain. Multiple reliability studies in adults have been conducted in fMRI and reported a wide range of reliability values, influenced by factors such as the duration of measurement, sample size, the frequency of task runs, and the specific tasks employed to assess reliability. The average reported reliability for task/rest fMRI at the individual level is generally low, with intraclass correlation coefficients (ICCs)³² often falling in the low and median range (between 0.2 to 0.6)^{33,34}. Similarly, other reliability studies on healthy adults have been conducted using EEG³⁵ and fNIRS^{36–39} to investigate reliability in imaging measurements. However, these studies^{36,40–43} have been often limited by small sample sizes, short quantities, single task or lab-based settings.

Our study aims to address these limitations by using an approach with multiple sessions in naturalistic settings (i.e., at-home and in-office) to improve the reliability and specificity of individual brain activity measurements during multiple cognitive tasks. Additionally, the neuroimaging assessments in our study were self-administered, which further enhances the ecological validity and scalability of our approach. To date, no fNIRS study has performed such dense-sampling measurements (total seventy minutes for each of four tasks). Our focus was on observing individualized connectivity patterns and brain activation across repeated sessions, aiming to assess both reproducibility and consistency of response. Our central hypothesis is that dense-sampled fNIRS data can improve the reliability and specificity of functional connectivity measures, laying the groundwork for identifying individualized patterns of brain activity. The aim of this study is to illustrate that repeated assessments of brain activity yield robust results within individuals and that an individual's brain data deviates from group-level averages. Moreover, we compare the similarity of brain maps at both group and individual levels, highlighting the importance of individualized neuroimaging for precise and accurate mapping of brain activity.

Results

Our platform incorporates a wireless, portable fNIRS headband designed for convenient use in users' homes alongside an intuitive tablet application for cognitive testing and wirelessly recording cortical activity (Fig. 1). Eight healthy young adults (5 females and 3 males, mean \pm SD age: 26.13 \pm 5.99) completed ten measurement sessions across three weeks. Each session, lasting approximately 45 min, included self-guided preparation and device placement, task explanations, practice, and cognitive testing. In each session, participants' brain data was recorded while they were performing N-back⁴⁴, Flanker⁴⁵, and Go/No-go⁴⁶ tests on the tablet as well as while they were resting (Supplementary Figs. 1 and 2). Each test lasted seven minutes and participants practiced each test with feedback before starting them.

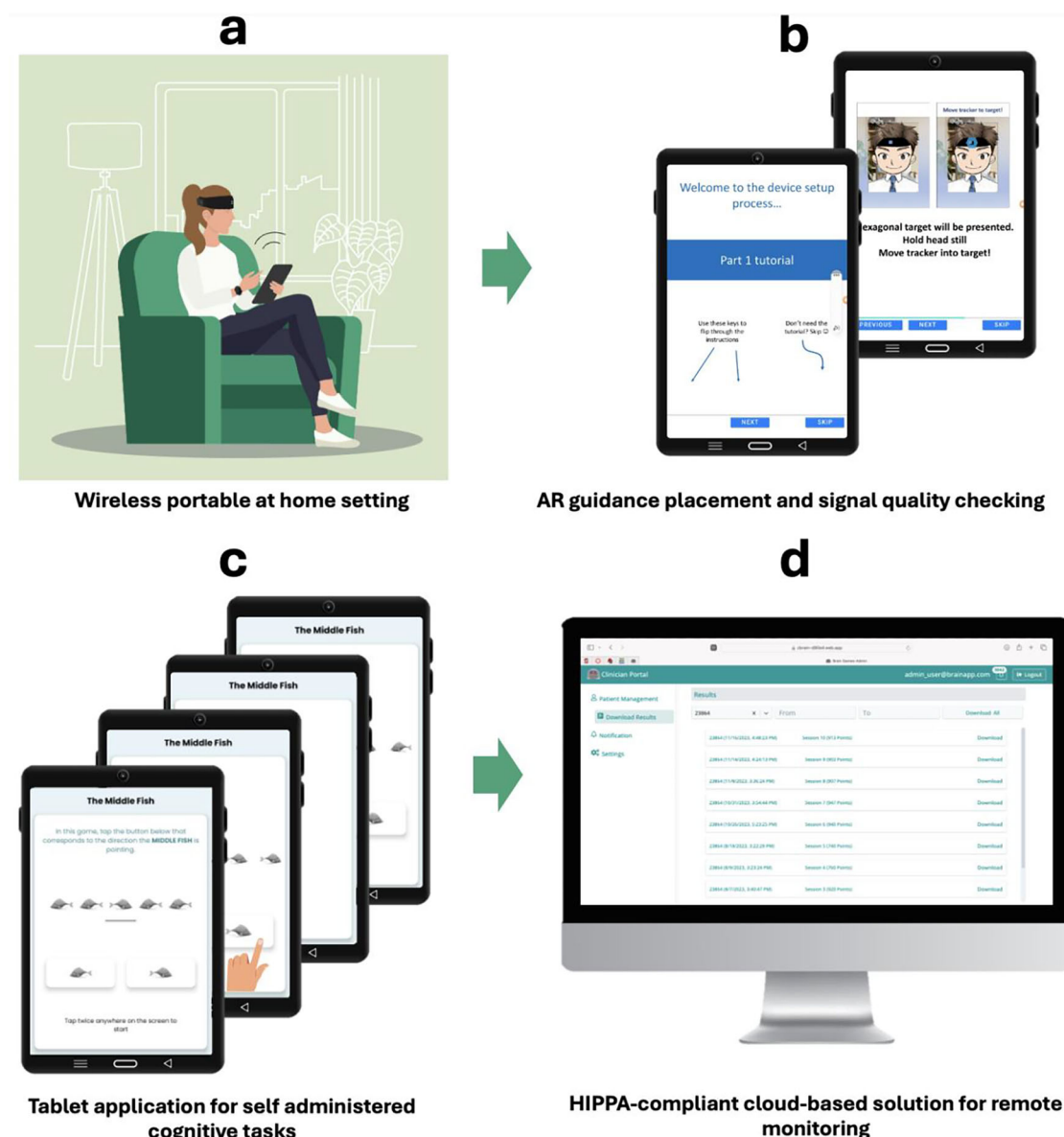


Fig. 1 | Our proposed fNIRS platform. The platform integrates (a) a 17-channel, wearable, wireless, portable fNIRS system used in a home or office setting and a tablet application that enables (b) proposed AR-guided placement of the device in a proper and reproducible manner, c wireless recording of brain activity while guiding the

user throughout a set of carefully designed cognitive tasks; and d a HIPAA-compliant, cloud solution for researchers to remotely manage users' brain response and cognitive outcomes. This setup highlights the modular design and the seamless integration of technology to enable self-administration and remote monitoring.

We analyzed the reliability and specificity of functional brain connectivity measured across the ten sessions at the individual level. We also examined individual-level and group-level functional brain activity of our dense-sampled oxygenated hemoglobin concentration (Oxy-Hb) and deoxygenated hemoglobin concentration (deoxy-Hb) data collected using our platform. In each of the eight participants, we collected 70 min (7 min per session across 10 sessions) of resting state fNIRS data and 210 min (21 min per session across 10 sessions) of task-based fNIRS data. The behavioral accuracy was consistently high in all individuals (averaged accuracy for N-back: $90\% \pm 6$; for Flanker: $92\% \pm 4$; for Go/No-go: $88\% \pm 8$).

Reliability

Test-retest reliability analyses for resting state functional connectivity (RSFC) and task-based functional connectivity (TBFC) measures were conducted for each individual and assessed based on the correlation of channel-to-channel connectivity matrices. Figure 2 illustrates that all measures exhibited relatively low reliability (as low as 0.25) given quantity of

one-session data (7 min). However, the reliability of additive measures increased sharply (up to 0.92) with inclusion of multiple data sessions (49 min). In two individuals (participants 2 & 3), reliability across the sessions in the Flanker task was relatively but not significantly lower due to motion artifacts; these individuals also showed the same trend of increasing reliability with more sessions.

Specificity

RSFC and TBFC matrix similarities were examined both within and across participants across all concatenated sessions⁴⁷. For all tasks, correlation matrix similarities were greater within participants than across participants (Fig. 3), indicating distinct individual RSFC and TBFC patterns. Besides, group-level t-statistics were computed to investigate functional connectivity across tasks (Fig. 4). Positive t-values ($T > 0$) indicate stronger connectivity in specific channel pairs, while negative t-values ($T < 0$) represent weaker connectivity. We observed significant positive functional connectivity ($p_{FDR} < 0.05$) for specific channel pairs including ch4-ch5 (right-left

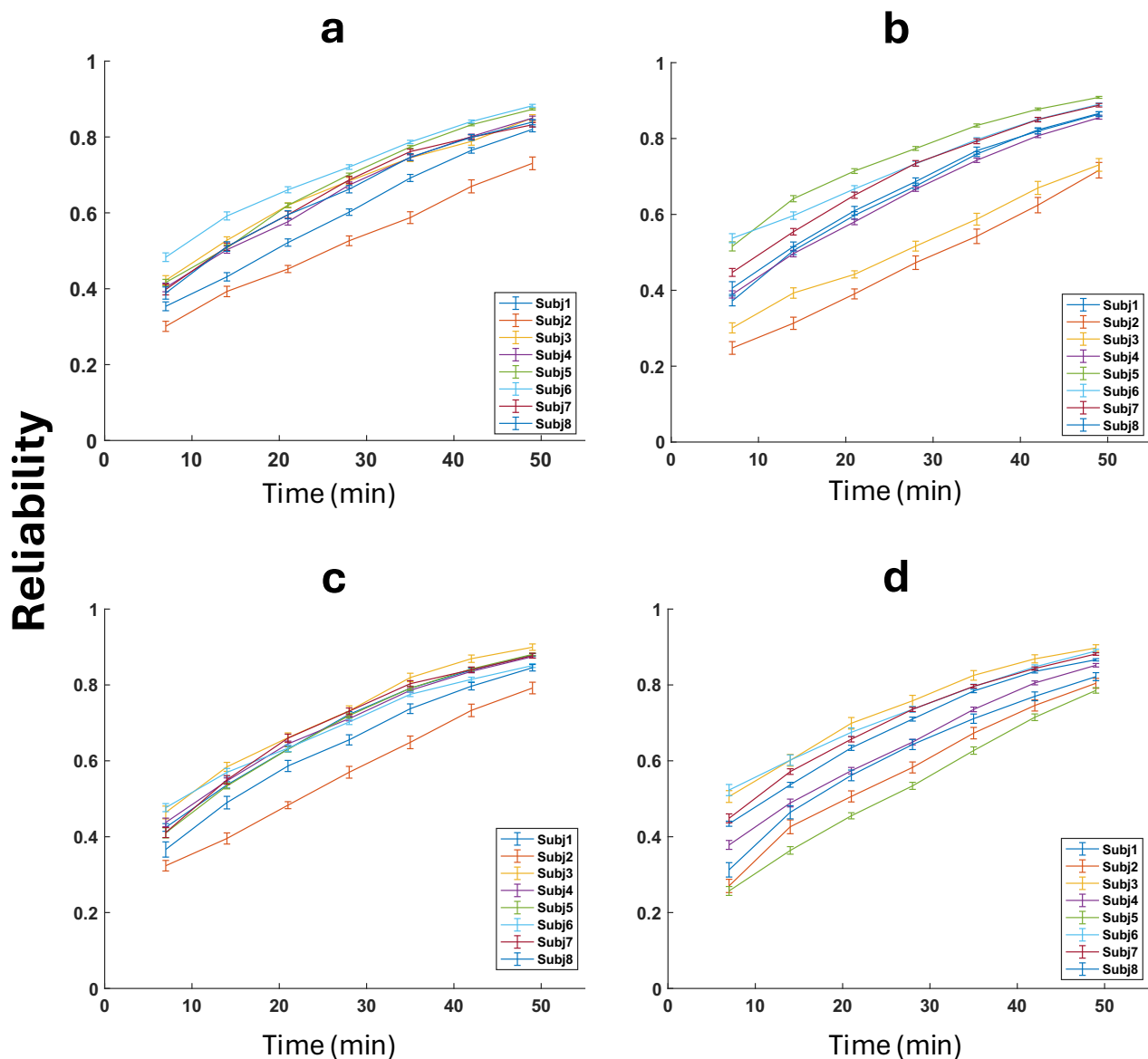


Fig. 2 | Changes in test-retest reliability of individual functional connectivity maps. Reliability is shown as a function of measurement length (7 to 49 min; 1 to 7 sessions) in eight healthy individuals during (a) N-back, b Flanker, c Go/No-go, and d resting state tasks. A given amount of data (from 7 min to 49 min)

was randomly selected and compared to a random independent sample of 49 min of data from the same participants in each task individually; this procedure was repeated 500 times using permutation testing.

dorsolateral PFC), ch6-ch7 (right-left lateral frontopolar cortex), ch7-ch8 (left lateral frontopolar cortex- medial PFC), ch10-ch14 (left ventrolateral PFC- right lateral frontopolar cortex) and ch11-ch13 (left-right orbitofrontal cortex).

Inter-subject variability was most prominent ($p_{FDR} < 0.05$) in channel pairs including ch2-ch7 (right ventrolateral PFC-left lateral frontopolar cortex), ch3-ch7 (right orbitofrontal cortex-left lateral frontopolar cortex), ch3-ch8 (right orbitofrontal cortex-medial PFC), and ch8-ch16 (medial PFC- left lateral frontopolar cortex) only within the N-back task (see Supplementary Fig. 3). More detailed representation is presented in Fig. 3 as within-participant RSFC and TBFC matrices, revealing individual-specific features of brain connectivity. Broad consistencies in within-participant connectivity were observed across the eight individuals, with significant connectivity in prefrontal channel pairs e.g., ch6-ch7 (right-left lateral frontopolar cortex), ch7-ch8 (left lateral frontopolar cortex- medial PFC), ch11-ch13 (left-right orbitofrontal cortex), ch8-ch16 (medial PFC- left lateral frontopolar cortex) consistent with group-average data (Fig. 4).

Overall, functional connectivity patterns observed across tasks predominantly involved interactions between the left and right lateral regions of the prefrontal cortex ($p_{FDR} < 0.05$). This observation underscores the potential role of hemispheric interactions in task-specific and resting-state connectivity, highlighting the prefrontal cortex's critical involvement in cognitive processes.

Pairwise comparisons of functional connectivity patterns across tasks were conducted using t-tests. While task-specific differences were observed in the t-statistics matrices (Supplementary Fig. 4), no channel pairs reached statistical significance after applying False Discovery Rate (FDR) correction ($p_{FDR} < 0.05$). This finding aligns with previous fMRI studies^{48–50} suggesting that resting-state connectivity often mirrors task-based connectivity due to the stability of intrinsic networks like the default mode network. The dense-sampling design across seven sessions provided robust individual network mapping but may have primarily reinforced these intrinsic patterns, limiting the detection of task-specific differences. These results emphasize the need for larger sample sizes and advanced analytical approaches to explore subtle differences in functional connectivity across cognitive states.

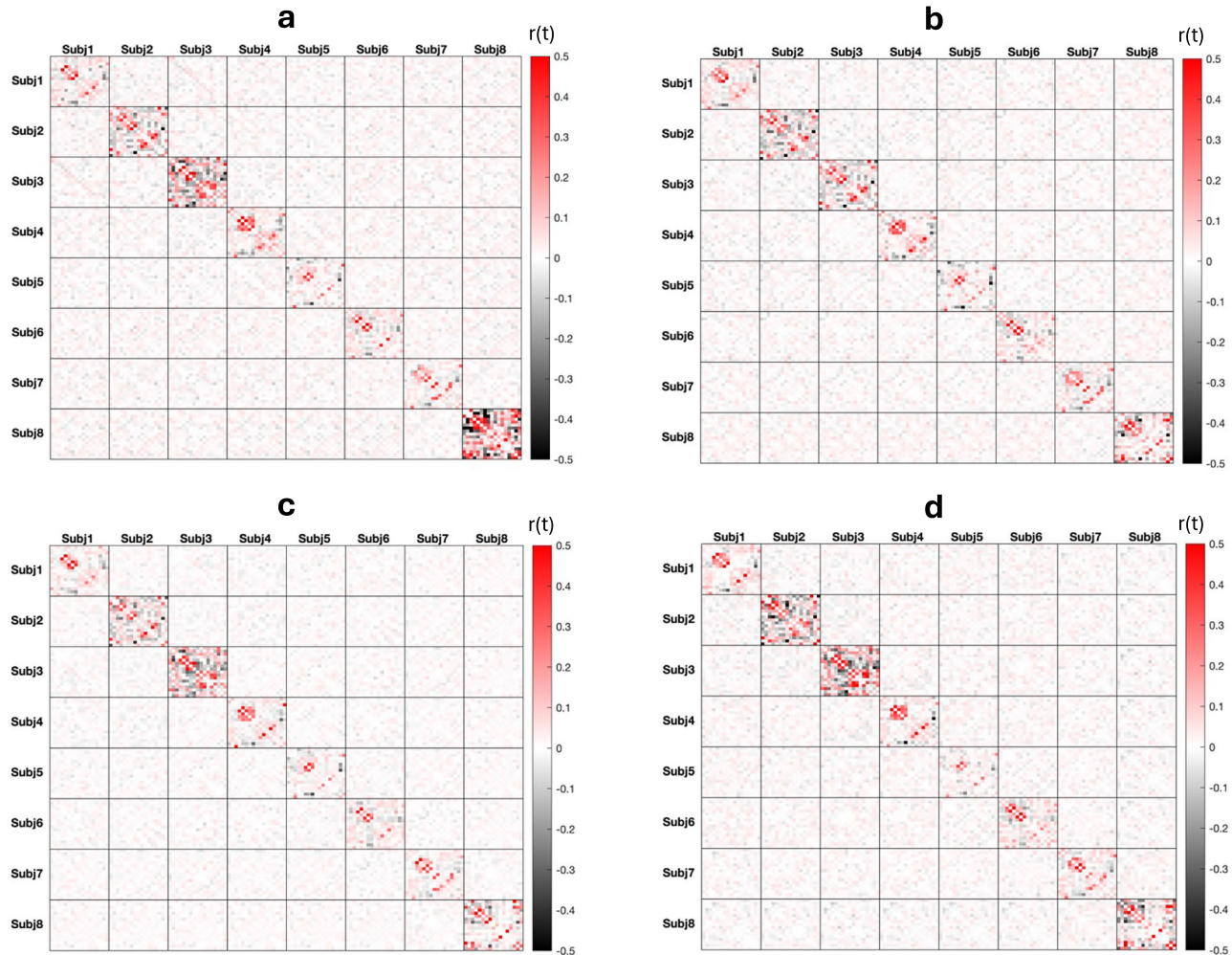


Fig. 3 | Specificity of individual functional connectivity patterns. Pairwise similarity of correlation matrices between all individuals, including all sessions, is shown in 8 healthy individuals during (a) N-back, b Flanker, c Go/No-go, and d resting state

tasks. This figure highlights the ability of the wearable platform to differentiate individual functional connectivity profiles across different cognitive states.

Individualized functional brain activity

Task-based fNIRS allows us to measure functional activity at both individual and group levels. Group-level fNIRS hemodynamic responses were examined using data from the first session as well as data from ten sessions concatenated. Concatenating data across all sessions resulted in group-average channel maps for each cognitive task that resulted in statistically significant activation and spatially specific, while analyzing data of only one session resulted in group-average maps with no statistically robust responses (Fig. 5). Particularly, no significantly active channel was observed in group averaged data of the first session for any of the tasks; however, we observed target activation consistent with previous studies^{51–53} in group-level maps of all concatenated sessions: (1) N-back: $t_{ch9(\text{left orbitofrontal cortex})} = 3.63, p_{FDR} = 0.01$. (2) Flanker: $t_{ch1(\text{right dorsolateral PFC})} = 1.78, p_{FDR} < 0.05$; $t_{ch9(\text{left orbitofrontal cortex})} = 3.38, p_{FDR} < 0.05$. (3) Go/No-go: $t_{ch13(\text{right orbitofrontal cortex})} = 3.44, p_{FDR} = 0.02$; $t_{ch11(\text{left lateral frontopolar cortex})} = 3.85, p_{FDR} = 0.01$.

As illustrated in Supplementary Fig. 5, individual Oxy-Hb revealed task-based activation inhomogeneity that was obscured by group averaging. More particularly, significant activations of specific prefrontal regions were observed in each individual that were mostly absent from the group average (discrepancy rate: 67%). A minimum four of eight participants (50%) had at least one channel with significant task-related activation ($p_{FDR} < 0.05$) in the prefrontal area in the first session; however, a minimum of seven participants (82.5%) showed at least one channel with significant task-related activation ($p_{FDR} < 0.05$) in concatenated sessions. Only one participant presents

the same significant spatial feature observed in the group-average activity.

To test if concatenating multiple sessions results in higher reproducibility, ICC was computed to assess the reliability of the observed functional activity for a single session across all ten sessions as well as for average of five (out of ten) interleaved sessions for each of the three cognitive tasks (Fig. 6). Approximately half of the channels showed above-good (>0.6) ICC for the concatenated interleaved sessions whereas only a few channels exhibited above-good ICCs for single-session analysis. More specifically, channel 13 (right orbitofrontal cortex) and channel 17 (left orbitofrontal cortex) during the N-back task, channel 1 (right dorsolateral PFC) during the Flanker task and channel 14 during the Go/No-go task demonstrated excellent ICC reliability in concatenated interleaved sessions. Interestingly, channels 1 (right dorsolateral PFC) and 14 (right lateral frontopolar cortex), which showed robust activation in group-level analysis, also exhibited an excellent level of ICC reliability in Flanker and Go/No-go tasks, respectively.

Discussion

Our study represents an initial step toward collecting dense-sampled fNIRS data, moving beyond the constraints of conventional neuroimaging studies in clinical psychiatry, which are typically confined to laboratory settings and limited to small-scale data collection^{3,7}. By enabling longitudinal monitoring of cortical activity across extended periods and diverse populations, our approach opens unprecedented opportunities for large-scale, real-world neuroimaging studies. These

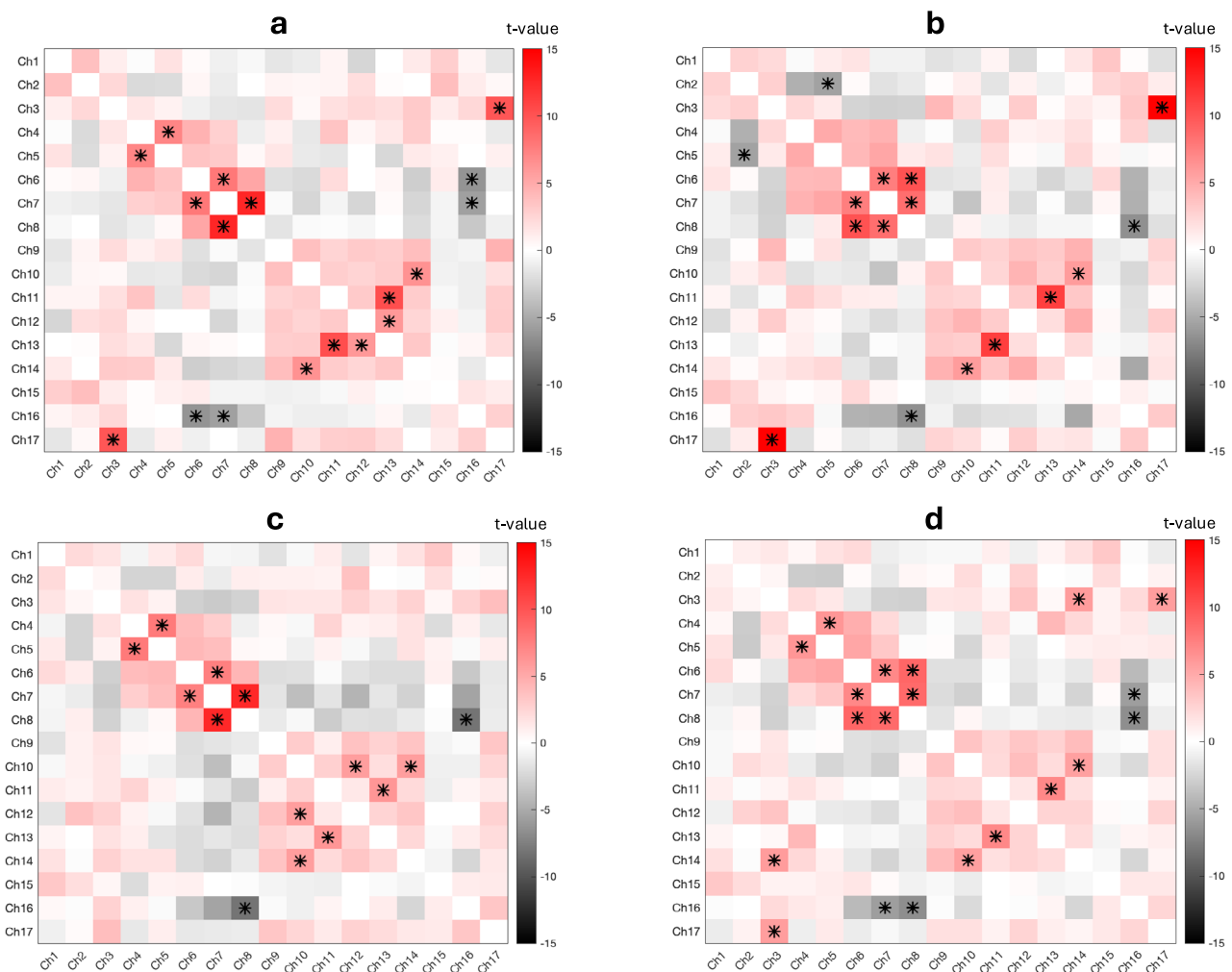


Fig. 4 | Group-Level T-Statistics matrix for functional connectivity across tasks. The figure displays the results of t-tests performed on Z-scores across all eight participants, highlighting significant group-level functional connectivity patterns for each task: **a** N-back; **b** Flanker; **c** Go/No-go; and **d** Resting state. Positive t-values

(red) indicate stronger group connectivity, while negative t-values (black) represent anti-correlation. Connections marked with an asterisk (*) denote statistically significant group effects at $p_{FDR} < 0.05$.

advancements lay a foundation for improving diagnostics, monitoring, and therapeutic interventions in mental health.

The wearable fNIRS platform demonstrated its potential as a cost-effective alternative to traditional neuroimaging methods. Its ability to collect dense-sampled data in naturalistic environments allows participants to engage in daily activities at home, overcoming the limitations of lab-based systems. These advancements enhance accessibility and reliability in functional neuroimaging. However, further validation is necessary to extend these findings beyond controlled environments.

The platform's reliability and innovative design hold promise for advancing psychiatric research: (1) Biomarker Identification: Dense-sampled data collection could enable the identification of reliable neurobiological biomarkers to complement subjective measures in mental health diagnostics. (2) Large-Scale Cohort Studies: The platform's low cost facilitates large-scale studies, capturing the heterogeneity of mental illnesses and uncovering new subtypes crucial for personalized treatment. (3) Ecological Validity: Collecting data in natural settings provides a more accurate representation of cortical activity patterns, which is critical for understanding real-world neural dynamics. (4) Clinical Applications: The platform can serve as a sensitive at-home outcome measure for monitoring treatment responses in clinical trials.

Dense sampling significantly improved reliability, with within-participant correlations increasing from 0.25 to 0.92 when aggregated

across sessions. This highlights the value of dense-sampled data for refining personalized neuroimaging strategies. Prefrontal connectivity associated with working memory, attention, and inhibition tasks showed high reliability, aligning with prior group-level fNIRS and fMRI findings^{54,55}. Targeted prefrontal sub-regions elicited from each cognitive task demonstrated high reliability, specificity, and robust activation in concatenated sessions and suggest the potential of using dense-sampled data to refine personalized neuroimaging strategies.

RSFC, TBFC, and task-based functional activity have enhanced our scientific understanding of human brain function. They have the potential to improve the clinical care of neurological, neurosurgical, and psychiatric patients beyond current presurgical planning applications. However, functional neuroimaging may not attain its full potential until very accurate individual-level brain activity estimates can be achieved^{12,54,56}. Our findings suggest that TBFC and RSFC-derived measures show promising reliability with sufficient data. These results align with prior fMRI studies illustrating the potential for stable connectivity patterns in single participants^{17,54}.

Functional connectivity analyses revealed predominantly interhemispheric connections in the prefrontal regions, including the dorsolateral, lateral frontopolar, and orbitofrontal cortices. These findings align with established literature emphasizing the role of interhemispheric communication in executive control and cognitive flexibility^{57,58}. Task-specific differentiation was limited, likely due to inadequate spatial resolution, small

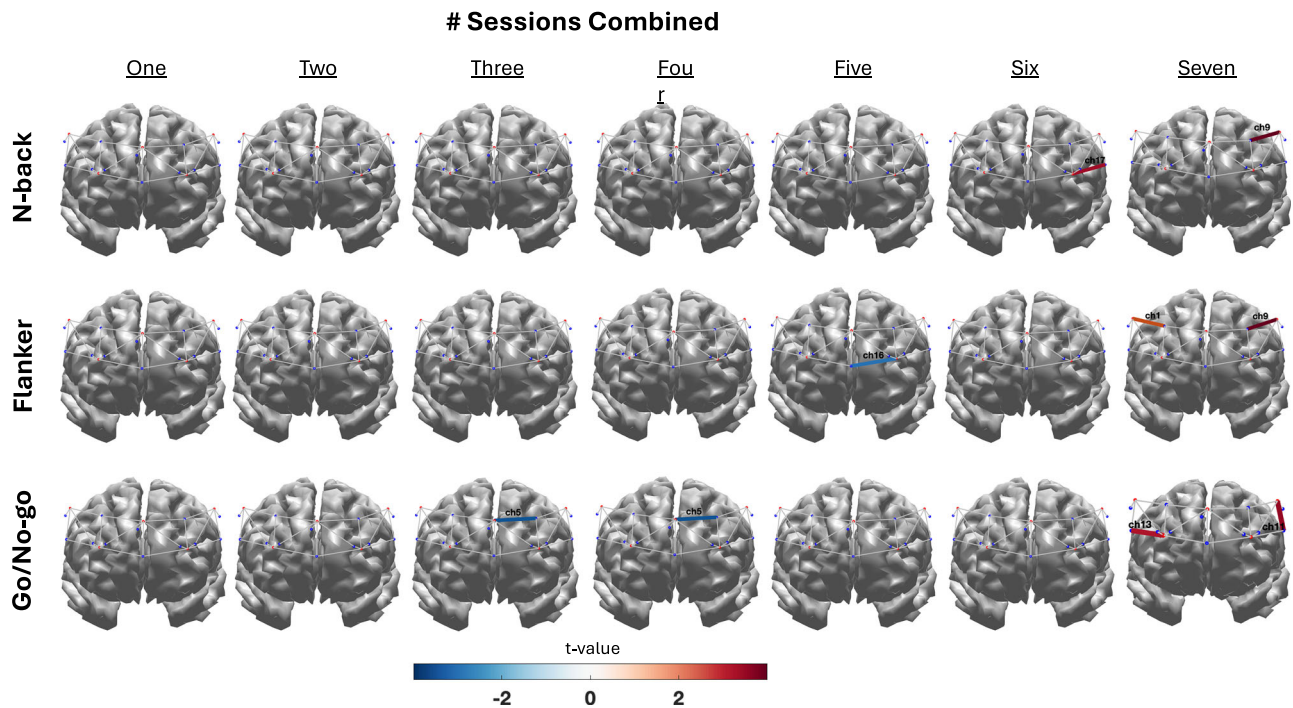


Fig. 5 | Significant group-level Oxy-Hb activation captured from the single session to seven combined sessions using dense-sampled fNIRS. The group-level activations are displayed from the single session to seven combined sessions, highlighting task-related prefrontal cortex activity. Channel maps represent significant Oxy-Hb activations during the N-back (1Back+2Back-0Back), Flanker, and

Go/No-go tasks, respectively. Please refer to Supplementary Fig. 5 for more detailed individual-level activations across one to seven concatenated sessions for all eight participants, demonstrating within-subject reliability and variability in task-based brain activation patterns.

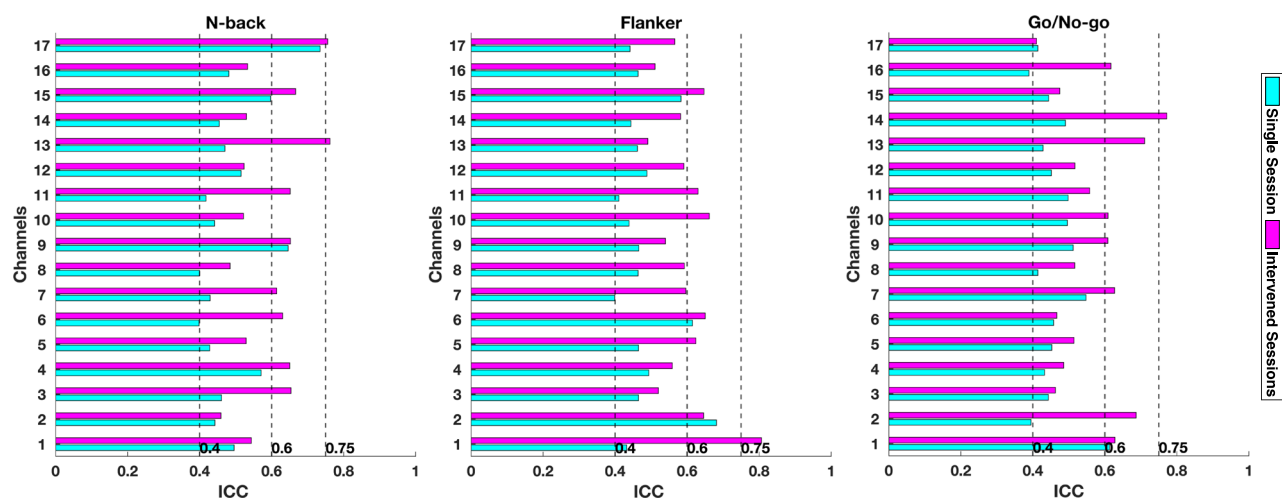


Fig. 6 | Reliability of functional activity across eight individuals. Reliability is shown for each of three cognitive tasks (N-back, Flanker, and Go/No-go) computed using the ICC of a single session and the average of interleaved sessions. Dashed line

segments depict different reliability thresholds as $0 < \text{poor} < 0.4$; $0.4 < \text{fair} < 0.6$; $0.6 < \text{good} < 0.75$; $0.75 < \text{excellent} < 1$.

sample size, and the shared reliance of tasks like N-back⁴⁴, Flanker⁴⁵, and Go/No-go⁴⁶ on overlapping prefrontal networks, particularly involving the dorsolateral PFC, ventrolateral PFC, orbitofrontal cortex, and medial PFC.

Precision mapping of individual brains reveals phenomena obscured by group averaging. Our results demonstrate how individual-specific brain activity violates the assumption of statistically consistent cortical activity across individuals for three executive functioning tasks, extending previous reports of individual-specific patterns absent from group-average analyses^{12,56,59}. Interestingly, some individual-specific activity patterns were frequently observed across the eight participants, though their functional significance is not yet clear.

Consistent with findings from fMRI studies^{48,49}, resting-state connectivity often predicted task-based connectivity^{11,12,54} due to shared intrinsic network structures, such as the default mode network. These networks exhibit high stability, which may obscure task-specific modulations, especially in small sample sizes. Dense sampling across sessions enhanced reliability within individuals but was insufficient to overcome inter-subject variability. Larger samples, targeted analyses, and complementary behavioral measures are necessary to distinguish task-specific patterns^{60–62}. Particularly, session-to-session similarities were high within participants but much lower across participants, consistent with connectivity-based “fingerprinting” findings in fMRI^{15,17,40,41}. These

differences may stem from spatial variations in brain activity, biological parameters (e.g., brain size), or non-biological factors (e.g., data quality, environmental conditions). Discriminating individuals thus requires extensive high-quality data^{11,12,54}.

This study's small sample size ($N = 8$) also limits the generalizability of findings. The lack of demographic diversity (e.g., Black participants) underscores the need for more inclusive cohorts to ensure broad applicability. Power analyses indicated that reliable brain-behavior correlations require significantly larger samples⁶³. Future research should expand cortical coverage, incorporate behavioral measures, and directly compare fNIRS and fMRI data under the same paradigms. Furthermore, our findings pave the way to investigate the association between activated regions for each cognitive task and corresponding RSFC measures, allowing functional annotation of activity features in each individual⁵⁵.

While this study did not explicitly assess participant comfort levels with the device and data acquisition process, informal feedback suggested that the wearable platform was generally well-tolerated, with no major discomfort reported during sessions. Future studies will include systematic assessments of participant comfort using standardized questionnaires to evaluate usability and identify any barriers to long-term or repeated use. These evaluations will guide refinements to the device design and data acquisition protocol to enhance the participant experience.

Collecting data in naturalistic settings introduces challenges, such as variability in environmental conditions and participant activities, which may introduce artifacts or confounders. Developing robust protocols for data collection (e.g., including self-reports), and daily life information (e.g., via ecological momentary assessments), preprocessing, and analysis (e.g., using advanced connectivity metrics⁶⁴ and machine learning techniques^{51–53,65,66}) is crucial to mitigate these factors. Future work should optimize the balance between ecological validity and experimental control to maximize the benefits of at-home data collection. Furthermore, while this study focused on evaluating the feasibility and reliability of a wearable fNIRS platform, it did not include an AR component. AR-guided device placement, a proposed feature of our platform, remains an important future direction that will be evaluated in follow-up studies. Additionally, our current findings lay the groundwork for future investigations in clinical populations. Specifically, we plan to extend this work to examine patient populations, such as individuals with neurodevelopmental disorders (e.g., ADHD), and assess the effects of medication and other interventions on functional brain connectivity. We also plan to integrate our platform with other wearable technologies, such as smartwatches, to achieve a more comprehensive understanding of physiological and brain function alterations in brain disorders.

This study highlights the reliability and precision of our wearable fNIRS platform for advancing mental health research. By performing preliminary analyses of multi-modal, dense-sampled, at-home brain monitoring, we demonstrated the platform's capability to reliably capture individualized patterns of functional connectivity and task-based brain activity. These findings are highly reproducible and emphasize the potential for wearable neuroimaging in personalized diagnostics and treatment planning. The observed differences in brain activity patterns across participants underscore the value of personalized neuroimaging for understanding individual variability. Individual RSFC and TBFC mappings revealed unique brain activity features, with functional connectivity predominantly observed between the left and right lateral prefrontal regions, emphasizing interhemispheric communication's critical role in cognitive processes. These insights reinforce the feasibility of wearable fNIRS platforms for individualized functional mapping.

The ability to collect extensive brain activity data in naturalistic settings represents a significant advancement over traditional lab-based neuroimaging studies, enabling large-scale population-level analyses. This approach provides a means to better capture the heterogeneity of mental illnesses, potentially identifying novel subtypes and generating hypotheses regarding their etiology. While further validation in larger and more diverse cohorts is required, the platform's capacity to produce reliable and

reproducible biomarkers highlights its potential applications in early detection and monitoring of mental illnesses, paving the way for improved treatments and outcomes.

Methods

Precision mental health platform

The custom-built fNIRS headband features five sources, each emitting near-infrared light at two different wavelengths (740 and 850 nm), and twelve detectors, resulting in 17 regular (source-detector separation: 2.8 cm) and 8 short channel measurements (source-detector separation: 0.9 cm) covering the prefrontal cortex area²⁷ (Detailed information is illustrated in Supplementary Fig. 6). The prefrontal cortex was chosen due to the focus on cognitive and executive functioning performance and the fact that these functions are impacted across mental illnesses⁴⁸. This platform facilitates wireless recording of brain activity and assists patients throughout the data collection process using an AR application⁴⁹, which tracks the headband's position and aligns it with the 10–20 standard placement for brain recordings. The integration of the AR-guided device placement was finalized after completing the data collection for this study, and thus, positioning of the headband during data collection for the present study was manual, following the standard 10–20 system as described in Rahimpour et al., 2020²⁵. The tablet application comprises four cognitive tasks administered in the following sequence: N-back, Flanker, Go/No-go, and resting state (See implemented tasks on the app in Supplementary Fig. 1). All data are securely stored in a HIPAA-compliant cloud solution, enabling remote management of patients' brain responses and cognitive outcomes with ease.

Channel configuration and signal correction

The channels in Supplementary Fig. 6 are not precisely equidistant (~2 mm) due to anatomical constraints of the wearable fNIRS headband. To address this, channel locations were determined based on the international 10–20 system, and their spatial positions were modeled using a 3D head model generated by NIRSite software. During data preprocessing, distance-dependent light attenuation was corrected using pathlength correction factors, ensuring comparability across channels despite variations in distance.

To ensure accurate device placement, the headband was manually positioned following the standard 10–20 system, with placement verified by trained researchers. Although the AR guidance feature was not utilized in this study, future implementations will incorporate this feature to provide real-time visual feedback for proper and reproducible placement, enhancing usability for non-experts. While participants did not receive direct feedback on data quality during sessions, researchers monitored signal quality at the start of each session using a built-in quality control module to ensure reliable data acquisition.

Participants

Eleven healthy adults (5 females, 6 males; aged 20–34 years, mean \pm SD = 28.11 \pm 5.422) consented to participate in the study. Three participants were excluded or lost to follow-up, primarily because they declined to continue and complete their ten sessions. Ultimately, eight participants successfully completed the trial (see demographic information in Supplementary Table 1). None of the participants reported any neurological disorder or injury that would prevent them from performing executive functioning tasks. This study was approved by the Stanford University School of Medicine Institutional Review Board for research ethics and human participants (Approval Reference Number: IRB-40332). Informed consent was obtained from all eight individual participants prior to their participation in the study. For all procedures, we adhered to the principles outlined in the Declaration of Helsinki and followed all relevant guidelines and regulations.

Experimental design and data acquisition

Participants underwent ten measurement sessions, each separated by a minimum of one day to minimize carryover effects. At the start of each

session, participants were seated in a quiet room at home (five participants) or at their office (three participants), instructed to minimize head movements, given the tablet with the application, and wore the fNIRS headband. The entire session, including fully self-guided instruction for participant preparation, task explanations, task practice, and actual task experiment lasted approximately 45 min. During each session, participants engaged in four different tasks: N-back, Flanker, Go/No-go, and resting state. Each task lasted 7 min, with a 10-s initial and final resting period included.

As shown in Supplementary Fig. 2, the N-back task comprised three levels (0-back, 1-back, 2-back; 10 trials for each level), each repeated four times. The task involved tapping on the screen based on specific number sequences. For the Flanker task, participants were presented with 60 stimuli of fish pointing either left or right and were required to select the correct direction using on-screen buttons. Stimuli included congruent and incongruent configurations with jittered interstimulus intervals of either 2, 5 or 7.5 s. For the Go/No-go task, a total of 168 trials were presented, consisting of Go (75%) and No-go (25%) trials. Participants tapped for specific alphabet letters (Go trials) and avoided tapping for the letter X (No-go trial), with non-trials (displayed as blank) introducing jittering. To avoid confusion, letters H, K, V, and Y were excluded from the Go trials because of their resemblance with letter X. Finally, participants were instructed to close their eyes and relax for seven minutes until they heard a noise for the resting state task, which served as a baseline for comparison.

Both behavioral and fNIRS data were collected during each session. Behavioral data included response times and accuracy, while fNIRS data measured prefrontal cortex activation. All parameters for each task remained constant across all sessions and participants. The experimental protocol was identical for each session, ensuring uniformity in data collection and analysis. This systematic approach aimed to gather comprehensive data on cognitive performance and prefrontal cortex activation across multiple sessions.

Rationale for task selection

The N-back, Flanker, and Go/No-go tasks were selected for their well-established role in assessing key components of executive functioning: working memory, attention, and response inhibition, respectively. These tasks have been extensively used in neuroimaging studies^{44,67,68}, including fNIRS and fMRI, and provide a robust framework for analyzing cortical activation patterns. Moreover, their reliable elicitation of prefrontal activation aligns with the PFC coverage of the fNIRS platform and the study's focus on executive functions. Their adaptability to a tablet-based interface further supports the feasibility of dense sampling in naturalistic settings.

Cognitive tasks were administered in a fixed order (N-back, Flanker, Go/No-go, and resting state), with a 10-second resting period between tasks to ensure consistency and comparability of task-related brain responses within and between participants. Besides, before the actual fNIRS measurements, participants practiced each task during every session using a feedback-enabled block. Once initiated, tasks were completed consecutively without interruption. However, future studies could benefit from incorporating a randomized task order. The app used in this study was designed for a predetermined task order; however, future iterations will integrate a randomized option to explore and account for potential order effects.

Data preprocessing

All data processing was performed in MATLAB using the Brain AnalyzIR toolbox⁶¹ in conjunction with custom code. The initial phase involved quality control to identify and exclude low-quality channels (each representing an ROI) for each session. Channels with Signal to Noise Ratio (SNR) below 20 dB and Quality Index (QI) below 0.5 were considered low quality and excluded from further analysis^{69,70}. The QI in this study refers to the Signal Cross-Correlation Index (SCI) as defined by Pollonini et al. (2016), which ranges from 0 to 1⁷¹. On average, 13 ± 4 high-quality channels (out of 17) were retained per session for subsequent analysis (see Supplementary Figs. 7 and 8 for hemoglobin data points and hemodynamic response functions).

Baseline corrections were applied to address direct current (DC) shifts, concatenation shifts, and the global signal. DC shifts were mitigated by subtracting the mean intensity over the baseline period for each channel, while concatenation shifts, caused by combining data across sessions, were corrected by aligning segments based on the mean signal value. To account for systemic physiological noise, the global signal was regressed out using the mean signal across all channels, isolating localized brain activity.

Furthermore, motion artifacts were addressed using wavelet filtering with the sym8 basis function from the family of wavelets refers to the 8th-order Symlet wavelet introduced by Ingrid Daubechies. This approach decomposed the fNIRS signal into frequency components, isolating and correcting motion-related artifacts. Instances deviating by more than 5 standard deviations from the mean were eliminated. Wavelet filtering is effective in addressing motion artifacts but has limited efficacy in handling very low-frequency noise. To mitigate this, additional baseline correction and high-pass filtering (cutoff frequency: 0.01 Hz) were applied to ensure the integrity of the data.

Finally, oxy-hemoglobin (Oxy-Hb) and deoxygenated hemoglobin (deoxy-Hb) concentrations were extracted using the modified Beer-Lambert law⁷². An age-dependent function was used for Differential Path-length Factor (DPF) calculation, accounting for age-related variations in tissue optical properties. This ensured accurate quantification of hemoglobin concentration changes^{73,74}. Oxy-Hb was prioritized for analysis due to its stronger correlation with BOLD fMRI signals⁷⁵.

Functional connectivity analysis

Functional connectivity was estimated using a robust regression approach that accounts for physiological noise and systemic artifacts. This method emphasizes reliable estimation of connectivity coefficients while minimizing the influence of external noise sources prior to constructing connectivity matrices. Individual functional connectivity was estimated on a channel-by-channel basis using an autoregressive partial correlation connectivity measure⁷⁶. This approach calculated the connectivity coefficients by assessing pairwise interactions across all channels, represented in individual connectivity matrices.

To further explore potential influences such as age and sex, robust linear regression models were applied to the connectivity data. Group-level connectivity analyses were conducted using only channels that consistently met the signal quality threshold (e.g., SCI > 0.5) across participants and sessions. On average, 76% of available channels were retained for analysis per participant, ensuring the reliability and comparability of results by using a standardized set of high-quality channels.

To calculate connectivity measures across all subjects and assess inter-subject variability, we utilized group-level t-statistics. Correlation coefficients (r values) for each subject were converted to Fisher's Z-scores to stabilize the variance of correlation coefficients. Subsequently, pairwise t-tests were conducted on the Fisher's Z-scores for each channel pair across all tasks to determine group-level connectivity patterns. This approach enabled the identification of significant connectivity differences and the assessment of inter-subject variability across the sample, providing a robust analysis of connectivity patterns.

Functional activity analysis

To improve signal fidelity and estimate regression coefficients, the AR-IRLS⁵⁸ regression model was implemented through the BrainAnalyzIR toolbox⁶¹. This step involved extracting data from short channels to minimize physiological and any extra motion-related artifacts, thereby enhancing the reliability of the fNIRS measurements⁶².

For subsequent statistical analysis, a general linear mixed regression model was employed to explore the effects of various factors on brain activation and connectivity. Independent variable included experimental tasks (N-Back, Flanker, Go-Nogo, and resting-state). The dependent variable, denoted as beta (β) represented the calculated coefficient for Oxy-Hb and deoxy-Hb for each specific condition. To minimize the risk of false positives, a correction procedure of the Benjamini-Hochberg method based

on the FDR was implemented. This correction method was applied to identify statistically significant channels ($P_{FDR} < 0.05$). By adjusting the p-values derived from the regression model, it was ensured that the reported significant channels had a minimal likelihood of being false positives.

Supplementary Fig. 8 illustrates the hemodynamic response functions (HRFs) generated using a general linear model (GLM)-based approach for each condition (1Back+2Back-0Back⁷⁷, Flanker, and Go/No-go tasks). The HRFs were estimated by regressing the oxy-hemoglobin concentration time series against task onsets convolved with a canonical HRF.

Reliability and specificity

The reliability of each functional connectivity measure (three cognitive tasks and one resting state) was assessed in each participant using an iterative comparison of random data subsets⁵⁴. For each participant, the 10 sessions were randomly split into two equal-sized, randomly selected subsets of sessions. Forty-nine minutes of data were randomly selected from one of the two subsets. A varying amount of data (ranging from one session: 7 min to five sessions: 49 min) was randomly selected from the other subset. Time courses from all 17 channels in the brain were used for generating the connectivity matrix, and then these connectivity maps were correlated against each other to calculate the reliability of RSFC and TBFC maps corresponding to the randomly selected subsets. To obtain robust estimates of the reliabilities of these measures for each participant, this procedure was iterated 500 times for each quantity of data tested, with a different random selection of data in each iteration.

To evaluate the within- and across-participant similarity of RSFC and TBFC measures, we calculated the pairwise similarity between all participant sessions. First, for each participant in each session, we generated a channel-to-channel RSFC and TBFC matrix using a common set of channels. The ‘common set of channels’ refers to channels that consistently passed the signal quality threshold ($SCI > 0.5$) across all participants and sessions. This approach ensured consistency and comparability in the connectivity analysis across sessions and individuals. We then calculated a similarity matrix by correlating each session’s functional connectivity matrix against all other sessions in all other participants. We then examined whether the similarities of sessions were higher within a participant than across participants.

We also measured Oxy-Hb for one session and the concatenation of multiple sessions at the individual level and group level for each cognitive task. We also investigated the effect of increasing the number of sessions on the target outcome and show the reliability resulted from multi-session inclusion based on task-based functional activity using ICC. We computed the ICC using the averaged AR-IRLS t-test statistics.

Data availability

Anonymized datasets will be made available from the corresponding author, HH, upon request (email: hosseiny@stanford.edu).

Code availability

The analysis scripts can be obtained upon request from the corresponding author, HH (email: hosseiny@stanford.edu).

Received: 21 September 2024; Accepted: 29 April 2025;

Published online: 13 May 2025

References

- Roehrig, C. Mental disorders top the list of the most costly conditions in The United States: \$201 Billion. *Health Aff.* **35**, 1130–1135 (2016).
- Bryce, S. et al. Cognitive health treatment priorities and preferences among young people with mental illness: the your mind, your choice survey. *Early Interv. Psychiatry* **18**, 94–101 (2024).
- Schultze-Lutter, F., Schmidt, S. J. & Theodoridou, A. Psychopathology—a precision tool in need of re-sharpening. *Front. psychiatry* **9**, 446 (2018).
- Brückl, T. M. et al. The biological classification of mental disorders (BeCOME) study: a protocol for an observational deep-phenotyping study for the identification of biological subtypes. *BMC Psychiatry* **20**, 1–25 (2020).
- Newson, J. J., Pastukh, V. & Thiagarajan, T. C. Poor Separation of Clinical Symptom Profiles by DSM-5 Disorder Criteria. *Front. Psychiatry* **12**, 775762 (2021).
- Feczko, E. et al. The heterogeneity problem: approaches to identify psychiatric subtypes. *Trends Cognit. Sci.* **23**, 584–601 (2019).
- The right treatment for each patient: unlocking the potential of personalized psychiatry. *Nat. Ment. Health* **1**, 607–608, <https://doi.org/10.1038/s44220-023-00131-y> (2023).
- Delgadillo, J. & Lutz, W. A development pathway towards precision mental health care. *JAMA Psychiatry* **77**, 889–890 (2020).
- Ng, M. Y. & Weisz, J. R. Annual research review: building a science of personalized intervention for youth mental health. *J. Child Psychol. Psychiatry* **57**, 216–236 (2016).
- Glover, G. H. Overview of functional magnetic resonance imaging. *Neurosurg. Clin. N. Am.* **22**, 133 (2011).
- Satterthwaite, T. D., Xia, C. H. & Bassett, D. S. Personalized neuroscience: common and individual-specific features in functional brain networks. *Neuron* **98**, 243–245 (2018).
- Gordon, E. M. et al. Precision functional mapping of individual human brains. *Neuron* **95**, 791–807 (2017).
- van Horn, J. D., Grafton, S. T. & Miller, M. B. Individual variability in brain activity: a nuisance or an opportunity?. *Brain Imaging Behav.* **2**, 327–334 (2008).
- Mueller, S. et al. Individual variability in functional connectivity architecture of the human brain. *Neuron* **77**, 586–595 (2013).
- Finn, E. S. et al. Can brain state be manipulated to emphasize individual differences in functional connectivity?. *Neuroimage* **160**, 140–151 (2017).
- Dubois, J. & Adolphs, R. Building a science of individual differences from fMRI. *Trends Cognit. Sci.* **20**, 425–443 (2016).
- Anderson, J. S., Ferguson, M. A., Lopez-Larson, M. & Yurgelun-Todd, D. Reproducibility of single-subject functional connectivity measurements. *AJNR Am. J. Neuroradiol.* **32**, 548 (2011).
- Highton, D., Boas, D. A., Minagawa, Y., Mesquita, R. C. & Gervain, J. Special section guest editorial: thirty years of functional near-infrared spectroscopy. **10**, 023501 (2023).
- Stute, K. et al. The fNIRS glossary project: a consensus-based resource for functional near-infrared spectroscopy terminology. <https://doi.org/10.31219/OSF.IO/7XN3B> (2024).
- Yücel, M. A. et al. The fNIRS Reproducibility Study Hub (FRESH): exploring variability and enhancing transparency in fNIRS neuroimaging research. <https://doi.org/10.31222/OSF.IO/PC6X8> (2024).
- Chen, W. L. et al. Functional near-infrared spectroscopy and its clinical application in the field of neuroscience: advances and future directions. *Front. Neurosci.* **14**, 540710 (2020).
- Pinti, P. et al. A review on the use of wearable functional near-infrared spectroscopy in naturalistic environments. *Jpn. Psychol. Res.* **60**, 347–373 (2018).
- Scarapicchia, V., Brown, C., Mayo, C. & Gawryluk, J. R. Functional magnetic resonance imaging and functional near-infrared spectroscopy: insights from combined recording studies. *Front. Hum. Neurosci.* **11**, 419 (2017).
- Klein, F., Debener, S., Witt, K. & Kranczioch, C. fMRI-based validation of continuous-wave fNIRS of supplementary motor area activation during motor execution and motor imagery. *Sci. Rep.* **12**, 1–20 (2022).
- Rahimpour, A., Pollonini, L., Comstock, D., Balasubramaniam, R. & Bortfeld, H. Tracking differential activation of primary and supplementary motor cortex across timing tasks: an fNIRS validation study. *J. Neurosci. Methods* **341**, 108790 (2020).

26. Cui, X., Bray, S., Bryant, D. M., Glover, G. H. & Reiss, A. L. A quantitative comparison of NIRS and fMRI across multiple cognitive tasks. *Neuroimage* **54**, 2808–2821 (2011).
27. Quaresima, V. & Ferrari, M. Functional Near-Infrared Spectroscopy (fNIRS) for assessing cerebral cortex function during human behavior in natural/social situations: a concise review. *Organ. Res. Methods* **22**, 46–68 (2019).
28. Tsuzuki, D. et al. Virtual spatial registration of stand-alone fNIRS data to MNI space. *Neuroimage* **34**, 1506–1518 (2007).
29. Tsow, F., Kumar, A., Hosseini, S. H. & Bowden, A. A low-cost, wearable, do-it-yourself functional near-infrared spectroscopy (DIY-fNIRS) headband. *HardwareX* **10**, e00204 (2021).
30. Noble, S., Scheinost, D. & Constable, R. T. A guide to the measurement and interpretation of fMRI test-retest reliability. *Curr. Opin. Behav. Sci.* **40**, 27–32 (2021).
31. Bennett, C. M. & Miller, M. B. fMRI reliability: influences of task and experimental design. *Cognit. Affect. Behav. Neurosci.* **13**, 690–702 (2013).
32. Koo, T. K. & Li, M. Y. A guideline of selecting and reporting intraclass correlation coefficients for reliability research. *J. Chiropr. Med.* **15**, 155–163 (2016).
33. Hassel, S. et al. Reliability of a functional magnetic resonance imaging task of emotional conflict in healthy participants. *Hum. Brain Mapp.* **41**, 1400–1415 (2020).
34. Wang, J. et al. Test-retest reliability of functional connectivity networks during naturalistic fMRI paradigms. *Hum. Brain Mapp.* **38**, 2226 (2017).
35. McEvoy, L. K., Smith, M. E. & Gevins, A. Test-retest reliability of cognitive EEG. *Clin. Neurophysiol.* **111**, 457–463 (2000).
36. Niu, H. et al. Test-retest reliability of graph metrics in functional brain networks: a resting-state fNIRS study. *PLoS ONE* **8**, e72425 (2013).
37. Blasi, A., Lloyd-Fox, S., Johnson, M. H. & Elwell, C. Test-retest reliability of functional near infrared spectroscopy in infants. *Neurophotonics* **1**, 025005 (2014).
38. Ranchet, M., Hoang, I., Derollepot, R. & Paire-Ficout, L. Between-sessions test-retest reliability of prefrontal cortical activity during usual walking in patients with Parkinson's disease: A fNIRS study. *Gait Posture* **103**, 99–105 (2023).
39. Huang, Y. et al. Test-retest reliability of the prefrontal response to affective pictures based on functional near-infrared spectroscopy. *J. Biomed. Opt.* **22**, 016011 (2017).
40. Uchitel, J., Blanco, B., Vidal-Rosas, E., Collins-Jones, L. & Cooper, R. J. Reliability and similarity of resting state functional connectivity networks imaged using wearable, high-density diffuse optical tomography in the home setting. *Neuroimage* **263**, 119663 (2022).
41. Plichta, M. M. et al. Event-related functional near-infrared spectroscopy (fNIRS): Are the measurements reliable?. *Neuroimage* **31**, 116–124 (2006).
42. Schecklmann, M., Ehlis, A. C., Plichta, M. M. & Fallgatter, A. J. Functional near-infrared spectroscopy: a long-term reliable tool for measuring brain activity during verbal fluency. *Neuroimage* **43**, 147–155 (2008).
43. de Rond, V. et al. Test-retest reliability of functional near-infrared spectroscopy during a finger-tapping and postural task in healthy older adults. *Neurophotonics* **10**, 025010 (2023).
44. Owen, A. M., McMillan, K. M., Laird, A. R. & Bullmore, E. N-back working memory paradigm: a meta-analysis of normative functional neuroimaging studies. *Hum. Brain Mapp.* **25**, 46–59 (2005).
45. Soares, S. M. P. et al. A diffusion model approach to analyzing performance on the Flanker task: The role of the DLPFC. *Biling. Lang. Cognit.* **22**, 1194–1208 (2019).
46. Simmonds, D. J., Pekar, J. J. & Mostofsky, S. H. Meta-analysis of Go/No-go tasks demonstrating that fMRI activation associated with response inhibition is task-dependent. *Neuropsychologia* **46**, 224–232 (2008).
47. Gordon, E. M. et al. Generation and evaluation of a cortical area parcellation from resting-state correlations. *Cereb. Cortex* **26**, 288–303 (2016).
48. Smith, S. M. et al. A positive-negative mode of population covariation links brain connectivity, demographics and behavior. *Nat. Neurosci.* **18**, 1565–1567 (2015).
49. Cole, M. W., Bassett, D. S., Power, J. D., Braver, T. S. & Petersen, S. E. Intrinsic and task-evoked network architectures of the human brain. *Neuron* **83**, 238–251 (2014).
50. Krienen, F. M., Thomas Yeo, B. T. & Buckner, R. L. Reconfigurable task-dependent functional coupling modes cluster around a core functional architecture. *Philos. Trans. R. Soc. B Biol. Sci.* **369**, 20130526 (2014).
51. Glasser, M. F. et al. A multi-modal parcellation of human cerebral cortex. *Nature* **536**, 171–178 (2016).
52. Greene, D. J. et al. Multivariate pattern classification of pediatric Tourette syndrome using functional connectivity MRI. *Dev. Sci.* **19**, 581–598 (2016).
53. Huth, A. G., De Heer, W. A., Griffiths, T. L., Theunissen, F. E. & Gallant, J. L. Natural speech reveals the semantic maps that tile human cerebral cortex. *Nature* **532**, 453–458 (2016).
54. Laumann, T. O. et al. Functional System and Areal Organization of a Highly Sampled Individual Human Brain. *Neuron* **87**, 657–670 (2015).
55. Tavor, I. et al. Task-free MRI predicts individual differences in brain activity during task performance. *Science* **352**, 216–220 (2016).
56. Harrison, S. J. et al. Large-scale probabilistic functional modes from resting state fMRI. *Neuroimage* **109**, 217–231 (2015).
57. Banich, M. T. The missing link: the role of interhemispheric interaction in attentional processing. *Brain Cognit.* **36**, 128–157 (1998).
58. Stephan, K. E., Fink, G. R. & Marshall, J. C. Mechanisms of hemispheric specialization: Insights from analyses of connectivity. *Neuropsychologia* **45**, 209 (2007).
59. Gordon, E. M. et al. Individual-specific features of brain systems identified with resting state functional correlations. *Neuroimage* **146**, 918–939 (2017).
60. Fuster, J. M. The prefrontal cortex - an update: time is of the essence. *Neuron* **30**, 319–333 (2001).
61. Santosa, H., Zhai, X., Fishburn, F. & Huppert, T. The NIRS brain AnalyzIR toolbox. *mdpi.com/H Santosa, X Zhai, F Fishburn, T Huppert/Algorithms*, <https://doi.org/10.3390/a11050073> (2018).
62. Gagnon, L. et al. Short separation channel location impacts the performance of short channel regression in NIRS. *Neuroimage* **59**, 2518–2528 (2012).
63. Marek, S. et al. Reproducible brain-wide association studies require thousands of individuals. *Nature* **603**, 654–660 (2022).
64. Hutchison, R. M. et al. Dynamic functional connectivity: promise, issues, and interpretations. *Neuroimage* **80**, 360–378 (2013).
65. Guntupalli, J. S. et al. A model of representational spaces in human cortex. *Cereb. Cortex* **26**, 2919–2934 (2016).
66. Langa, G. et al. Identifying shared brain networks in individuals by decoupling functional and anatomical variability. *Cereb. Cortex* **26**, 4004–4014 (2016).
67. Lloyd-Fox, S., Blasi, A. & Elwell, C. E. Illuminating the developing brain: the past, present and future of functional near infrared spectroscopy. *Neurosci. Biobehav. Rev.* **34**, 269–284 (2010).
68. Scholkmann, F. et al. A review on continuous wave functional near-infrared spectroscopy and imaging instrumentation and methodology. *Neuroimage* **85**, 6–27 (2014).
69. Yücel, M. A. et al. Best practices for fNIRS publications. *Neurophotonics* **8**, 012101 (2021).
70. Hernandez, S. M. & Pollonini, L. NIRSplot: a tool for quality assessment of fNIRS scans. *Optics and the Brain, BM2C-5* (2020).
71. Pollonini, L. et al. PHOEBE: a method for real time mapping of optodes-scalp coupling in functional near-infrared spectroscopy. *Biomed. Opt. Express* **7**, 5104 (2016).

72. Kocsis, L., Herman, P. & Eke, A. The modified Beer–Lambert law revisited. *Phys. Med. Biol.* **51**, N91 (2006).
73. Scholkmann, F., Metz A. J., & Wolf, M. Measuring tissue hemodynamics and oxygenation by continuous-wave functional near-infrared spectroscopy---how robust are the different calculation methods against movement artifacts? <https://doi.org/10.1088/0967-3334/35/4/717>.
74. Duncan, A. et al. Measurement of cranial optical path length as a function of age using phase resolved near infrared spectroscopy. *Pediatr. Res.* **39**, 889–894 (1996).
75. Strangman, G., Culver, J. P., Thompson, J. H. & Boas, D. A. A quantitative comparison of simultaneous BOLD fMRI and NIRS recordings during functional brain activation. *Neuroimage* **17**, 719–731 (2002).
76. Lanka, P., Bortfeld, H. & Huppert, T. J. Correction of global physiology in resting-state functional near-infrared spectroscopy. *Neurophotonics* **9**, 035003 (2022).
77. Rahimpour Jounghani, A. et al. Neuromonitoring-guided working memory intervention in children with ADHD. *iScience* **27**, 111087 (2024).

Acknowledgements

This study was partly funded by National Institute of Mental Health (R21MH123873). A.R.J.'s effort was supported in part by NIH T32 fellowship (5T32MH019908). A.K.B.'s effort was supported in part by Dorothy J Wingfield Phillips Chancellor Faculty Fellowship. L.M.C.'s effort was partly supported by the La Caixa Banking Foundation Fellowship.

Author contributions

ARJ: Conceptualization, Methodology, Formal analysis, Visualization, Data curation, Writing - original draft, Writing- review & editing. AK: Conceptualization – technology, Technology design & development, Software Development. LMC: Methodology, Visualization, Data curation, Writing- review & editing. EPA: Visualization, Data curation, Writing- review & editing. TP: Visualization, Data curation. SC: Technology development. AKB: Conceptualization – technology, Technology design and development, Resources, Writing – review & editing, Funding acquisition. HH: Conceptualization, Methodology, Platform and technology design, Study design, Resources, Writing - review & editing, Funding acquisition.

Competing interests

A.K. and H.H. have a financial interest in Walnot, Inc. which may benefit from the results of this research. The remaining authors declare no competing interests.

Additional information

Supplementary information The online version contains supplementary material available at <https://doi.org/10.1038/s41746-025-01690-3>.

Correspondence and requests for materials should be addressed to S. M. Hadi Hosseini.

Reprints and permissions information is available at <http://www.nature.com/reprints>

Publisher's note Springer Nature remains neutral with regard to jurisdictional claims in published maps and institutional affiliations.

Open Access This article is licensed under a Creative Commons Attribution-NonCommercial-NoDerivatives 4.0 International License, which permits any non-commercial use, sharing, distribution and reproduction in any medium or format, as long as you give appropriate credit to the original author(s) and the source, provide a link to the Creative Commons licence, and indicate if you modified the licensed material. You do not have permission under this licence to share adapted material derived from this article or parts of it. The images or other third party material in this article are included in the article's Creative Commons licence, unless indicated otherwise in a credit line to the material. If material is not included in the article's Creative Commons licence and your intended use is not permitted by statutory regulation or exceeds the permitted use, you will need to obtain permission directly from the copyright holder. To view a copy of this licence, visit <http://creativecommons.org/licenses/by-nc-nd/4.0/>.

© The Author(s) 2025